COLLOIDAL PROCESSING AND SOME PROPERTIES OF ALUMINA DISPERSED TETRAGONAL ZIRCONIA

Satoshi Akutsu*, Yoshio Sakka**, Tohru S. Suzuki**, Keijiro Hiraga** and Shigeru Ito*

*Science University of Tokyo, Faculty of Science and Technology, 2641 Yamasaki, Noda, Chiba 278-8510

** National Research Institute for Metals, 1-2-1, Sengen, Tsukuba, Ibaraki 305-0047
Fax: 0298-59-2401, e-mail:ysakka@nrim.go.jp

Al_2O_3 dispersed tetragonal ZrO_2 (3mol% Y_2O_3 doped ZrO_2) compacts were produced by colloidal process. Dispersed aqueous suspensions consisting of ZrO_2 and Al_2O_3 fine particles were prepared by the adsorption of polyelectrolyte on the particle surface. The compacts, consolidated by slip casting and cold isostatic pressing (CIP), were sintered at temperatures from 1000℃ to 1600℃. Densification was enhanced when Al_2O_3 content was up to 10vol%. The electric conductivity of the compacts when sintered at 1400 and 1600℃ was measured with an ac current complex impedance method. The bulk conductivities decreased with increasing Al_2O_3 content, but grain boundary conductivities took maximum values. Tensile strength was also measured for the samples sintered at 1300℃ and excellent tensile elongation was confirmed.
Key words: tetragonal zirconia, alumina, colloidal processing, ionic conductivity, superplasticity

1. INTRODUCTION

Sintered ceramics with fine particle size can have very interesting properties, such as excellent strength, hardness, high-temperature ductility, etc. [1, 2]. In order to obtain a fine particle size after sintering, fine particles must be used at the powdered stage as the precursor making. However, particles of submicron size are difficult to disperse uniformly in conventional dry processing technique. For particles dispersed in liquid suspension it is useful to use colloidal processing for consolidation to the solid form [3-5]. This is a very effective method for producing a uniform distribution of particles, and the creation of high-density ceramics.

In this study, colloidal processing was applied for a two phases heterogenous microstructure to demonstrate the effects of a uniform distribution of fine Al_2O_3 particles on the properties of tetragonal ZrO_2. Y_2O_3-doped tetragonal ZrO_2 is known to show high ionic conductivity [6] and excellent mechanical properties [7]. Al_2O_3 was added for possible improvements in sintering, ionic conductivity [8, 9] and high temperature ductility for t-ZrO_2.

2. EXPERIMENTAL

The α-Al_2O_3 and γ-Al_2O_3 powders used in this study were high-purity Al_2O_3 produced by Taimei Chemical Ltd.(TM-DAR, TM-70). The ZrO_2 powder was 3mol% Y_2O_3 stabilized tetragonal ZrO_2 (Tosoh: TZ3Y). The powders, α - and γ -$Al_2O_3$and TZ3Y, were 0.2, 0.02 and 0.07 μm, respectively in mean particle size. When suspensions consist of particles of different size and density, long range segregation is caused by differences in the rate of sedimentation during slip casting [10]. It has been confirmed that such segregation is prevented if the solid content of a suspension is more than 30vol% [11]. Therefore,

aqueous suspensions containing 30vol% solids were prepared for the composition of TZ3Y-0~70vol% α - Al_2O_3 and TZ3Y-0~23vol% γ - Al_2O_3.

Although a fine microstructure is expected when suspension containing fine particles is used, re-dispersion is needed to properly disperse a mixture of fine particles because of their weak agglomeration [12]. The suspensions were ultrasonicated for 10 min and stirred with a magnetic stirrer for over 12 h at room temperature to disperse the Al_2O_3 and TZ3Y particles homogeneously. Sufficient polyelectrolyte (poly (ammonium acrylate), Toa Gohsei, ALON A-6114) was added to the suspensions to maintain the particle dispersion. Rheological characteristics of the suspensions were measured by a cone and plate viscometer (Toki Sangyo, RC-500). After evacuation in a desicator to eliminate air bubbles, the suspension was consolidated by slip casting. The green compacts obtained by slip casting were treated by cold isostatic pressing (CIP) at 400MPa, followed by sintering at 1200, 1300, 1400 and 1600℃ for 2h in air.

The pore size distribution of the as-slip cast and CIPed compacts was measured with a mercury porosimeter (Micrometrics, AUTOPORE II9220). The size distribution was calculated using standard values of the mercury surface energy (0.48 N/m) and the contact angle (140 degree). The densities of the green and sintered bodies were measured by the Archimedes' method using kerosene. The microstructures of the sintered specimens were observed by SEM on polished and thermally etched surfaces.

The electric conductivity of the compacts sintered at 1400℃ and 1600℃ was measured with an ac current complex impedance method over the frequency range of 100 Hz to 15 MHz. Tensile tests were conducted on the sample

sintered at 1300℃ with a gauge dimension of 9 (length)-3.5 (wide)-3 (thickness) mm.

3. RESULTS AND DISCUSSION

The van der Waals force, buoyancy, gravity, and the electrostatic force act on particles in suspensions. The dispersion (or flocculation) behavior of a suspension used for colloidal processing is determined from the interaction energy which is the sum of the van der Waals and electrostatic repulsion forces. The measured results for the ζ-potential of the TZ3Y and Al_2O_3 powder used in this experiment are shown in Fig.1 as a function of pH. The effects of adding polyelectrolyte on both powders are also shown. If the pH is changed to strongly acidic or alkaline condition, a substantial electrostatic charge will develop on the surface of Al_2O_3 and TZ3Y particles. If this surface electric charge becomes large, then the potential energy of repulsion will also become large and a good dispersion of particle can be expected. The ζ-potential was found to increase in the alkaline condition when polyelectrolyte was added to the suspension. This effect is caused by polyelectrolyte molecules adhering to the surface of the particles, dissociating and increasing the potential. Furthermore, polyelectrolyte adsorbed on the particle surface acts as a solid obstacle to prevent flocculation, while also assists the dispersion in the suspension. The pH of the suspensions for the added polyelectrolyte by this
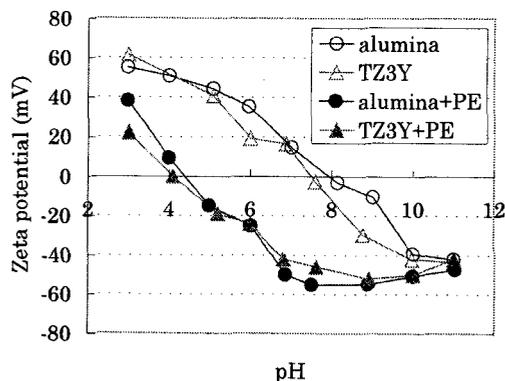
Fig.1 Relation between zeta potential and pH for alumina and TZ3Y particles, where PE indicates adding appropriate amount of polyelectrolyte.

Fig.3 Pore size distributions of as-slip casting compacts.

experiment was approximately 9.5.

Figure 2 shows the relative density of the compacts after slip casting and following CIP treatment plotted as Al_2O_3 content. In Fig.2(a), the relative density is high and takes a constant value as the volume fraction of α-Al_2O_3 is increased. In Fig.2(b), however, the relative density of the as-slip cast compacts decreased as the volume fraction of γ-Al_2O_3 was increased. In both cases the CIP treatment is very effective to improve the green density. In order to explain the different packing characteristics of the alumina powders, the pore radius distribution was measured for the compacts containing TZ3Y, α-Al_2O_3 and γ-Al_2O_3. These results are shown in Fig.3. The sharp peak in the pore radius for the primary particle is only observed for the TZ3Y and α-Al_2O_3 compacts. This result shows that the particle distribution is uniform for the TZ3Y and α-Al_2O_3 powders. However, for the γ-Al_2O_3 compacts, the size primary pores is close to 0.01 μ m, and that of secondary and tertiary pores, arising due to the coagulation of the primary particles, is close to 0.03 μ m. Therefore, for the γ-Al_2O_3 particles we can surmise that a uniform distribution is not achieved. This is why the relative density of the as-slip cast compacts decreases with γ-Al_2O_3. Here, the volume of the secondary and tertiary pores decreases in CIP treatment, and the relative density increases.

Fig.2. Relative densities of slip casted and CIPed compacts plotted as a function of Al_2O_3 content (α-Al_2O_3 (a) , γ-Al_2O_3 (b)).
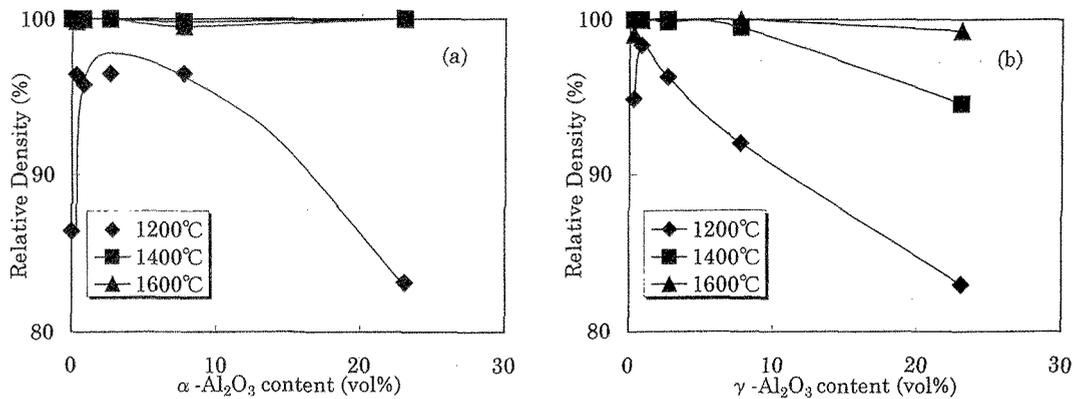
Fig.4. Relative densities of sintered compacts plotted as a function of Al_2O_3 contents (α-Al_2O_3 (a), γ-Al_2O_3 (b)).

The relative densities of the sintered bodies are shown in Fig. 4. When the α- and γ-Al_2O_3 additions were increased to 10 vol%, the relative densities of the sintered bodies increase compared to the TZ3Y without Al_2O_3 addition. For the same sintering temperature, comparing the relative densities of TZ3Y with α-Al_2O_3 addition and TZ3Y with γ-Al_2O_3 addition, it can be seen that the relative density of TZ3Y with γ-Al_2O_3 addition is low. This result is due to γ-Al_2O_3 particle coagulation as described above.

Figure 5 shows SEM photographs of polished and thermal etched surfaces of 7.7 vol% Al_2O_3
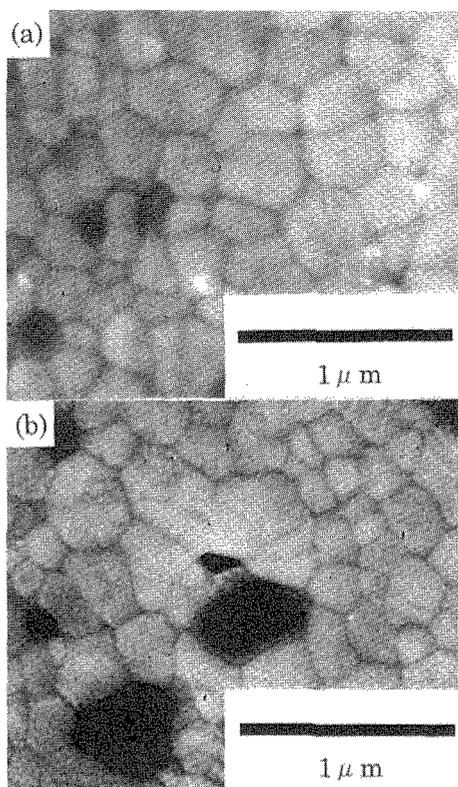
Fig.5. SEM micrographs of 7.7 vol% α-Al_2O_3dispersed (a) and γ-Al_2O_3 dispersed (b) TZ3Y sintered at 1400℃, where black parts are Al_2O_3 grains.

dispersed TZ3Y samples sintered at 1400℃. The grain size of TZ3Y in both samples dispersed by 7.7 vol% α-Al_2O_3 and γ-Al_2O_3 was about 0.3 μm. However, the grain size of the dispersed Al_2O_3 was different; the size of the Al_2O_3 phase from the γ-$Al_2O_3$was about 0.4 μm but that from the α-Al_2O_3 was about 0.2 μm. It is confirmed that the γ-Al_2O_3 particles coagulated not only from the results of Fig.3 but also from the SEM observation. Therefore, conductivity property and tensile elongation were measured for the α-Al_2O_3 dispersed samples.

Conductivity measurements were conducted for the samples of α-Al_2O_3 dispersed TZ3Y sintered at 1400℃ and 1600℃. From complex impedance spectra (Cole-Cole plots), bulk and grain boundary conductivities were separately determined. Figure 6 shows effect of Al_2O_3 addition on the bulk and grain boundary conductivities measured at 350 ℃. The bulk conductivities of both samples are similar but decrease with increase of Al_2O_3 addition. However, the grain boundary conductivities of both samples increase up to 7.7 vol% Al_2O_3 addition. An explanation is that the grain
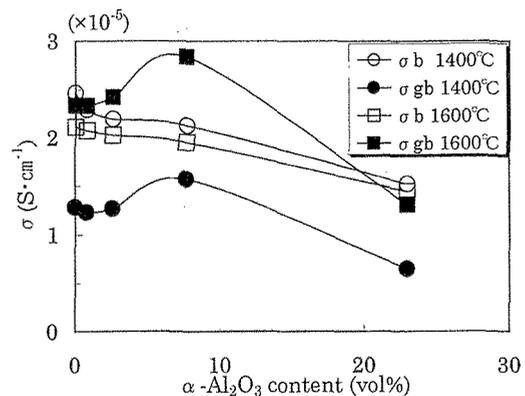
Fig.6.Effect of alumina addition on bulk and grain boundary conductivities for the samples sintered at 1400 and 1600℃
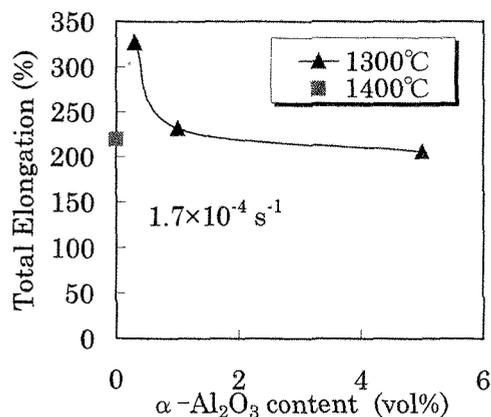
Fig.7 Effect of Al_2O_3 addition on tensile
elongation of TZ3Y samples.

boundary phase enriched by yttria and impurity silica is cleaned [8] due to the reaction of the grain boundary phase with α-Al_2O_3. The higher grain boundary conductivity of the sample sintered at 1600 °C than that at 1400 °C is explained by the brick-layer model [13,14]. The specific bulk conductivity σ_b (sp) and the specific grain boundary conductivity σ_{gb} (sp) are given as follows: σ_b (sp) $= \sigma_b$, and σ_{gb} (sp)$= \sigma_{gb} \cdot (\delta_{gb} / a)$, where δ_{gb} is the effective electrical thickness of the grain boundary and a (=0.806x(grain size)) the edge length of the cubic grains. If the grain boundary thicknesses of both samples are the same, the specific grain boundary conductivities of both samples are similar by considering the difference among the grain sizes, where the grain sizes of the TZ3Y sintered at 1400°C are in the range of 0.3-0.4 μm, but those at 1600°C are in the range of 0.7-0.9 μm.

Figure 7 shows effect of Al_2O_3 addition on the tensile elongation at an initial strain rate of 1.7 x 10^{-4} s^{-1}. Here, it is noted that the undoped sample was examined at 1400°C but the Al_2O_3 dispersed samples at 1300°C. Significant improvement of the tensile ductility of the 3YTZ samples was confirmed by small amount of Al_2O_3 addition. To determine the mechanism of the tensile elongation experiments on the tensile flow stress exponent and activation energy of tensile creep are now in progress.

4. SUMMARY

Homogeneous and fine-grained Al_2O_3 dispersed TZP was prepared by colloidal processing. The bulk conductivities of both samples sintered at 1400 and 1600°C are similar but decrease with increase of Al_2O_3 addition. However, the grain boundary conductivities of both samples increase at 7.7 vol% α-Al_2O_3 addition, which is explained by the brick-layer model. Excellent superplastic property was observed for Al_2O_3 dispersed TZP sintered at 1300°C.

References

[1] F. Wakai, S. Sakaguchi and Y. Matsuno: Advanced Ceramic Materials 1 (1986), pp. 259.
[2] M. J.-Melendo, A. D-Rodriguez and A. B-Leon:, J. Am. Ceram. Soc. 81 (1998), pp. 2761.
[3] F. F. Lange: J. Am. Ceram. Soc. 72 (1989), pp. 3.
[4] I. A. Aksay: Ceramic International 17 (1991), pp. 267.
[5] T. Uchikoshi, Y. Sakka, K. Ozawa and K. Hiraga: J. Europ. Ceram. Soc. 5 (1998), pp. 2123.
[6] N. Bonanos, R. K. Slotwinski and B. C. H. Steele: J. Mater. Sc. Lett. 4 (1985), pp. 487.
[7] T. Tsukuma, K. Ueda and M. Shimada: J. Am. Ceram. Soc. 68 (1985), pp.C-4.
[8] J. Drennan and S.P.S. Badwal: Advances in Ceramics 24 (1988), pp. 807.
[9] K. Oe, K. Kikkawa, A. Kishimoto, Y. Nakamura and H. Yanagida: Solid State Ionics 91 (1996), pp. 131.
[10] Y. Hirata and I. A. Aksay: pp.3-15 in Advances in Materials, Processing and Manufacturing, Proceedings of the Advanced Materials Technology Ceramic Workshop, No. 4. International Committee for Advanced Materials Technology, Nagoya, Japan, 1988.
[11] T. S. Suzuki, Y. Sakka and K. Hiraga: J. Jpn. Soc. Powder and Powder Metall. 44 (1997), pp. 356.
[12] T. S. Suzuki, Y. Sakka, K. Nakano and K. Hiraga: Mater. Trans., JIM 39 (1998), pp. 689.
[13] S.P.S. Badwall and J. Drennan: J. Mater. Sci. 22 (1987), pp. 3231.
[14] M. Aoki, Y. -M. Chiang, I. Kosacki, J. -R. Lee, H. Tuller and Y. Liu: J. Am. Ceram. Soc. 79 (1996), pp. 1169.